

Interplay between orbital ordering and lattice distortions in LaMnO_3 , YVO_3 , and YTiO_3

T. Mizokawa, D. I. Khomskii, and G. A. Sawatzky

Solid State Physics Laboratory, Materials Science Centre, University of Groningen, Nijenborgh 4, 9747 AG Groningen, The Netherlands

(March 21, 2022)

We have studied the interplay between orbital ordering, Jahn-Teller and GdFeO_3 -type lattice distortions in perovskite-type transition-metal oxides using model Hartree-Fock calculations. It has been found that the covalency between A -site cations and oxygens causes interaction between the Jahn-Teller and GdFeO_3 -type distortions. The present calculations explain why the d -type Jahn-Teller distortion and orbital ordering compatible with it are realized in LaMnO_3 , YVO_3 and YTiO_3 .

I. INTRODUCTION

Orbital ordering and concomitant Jahn-Teller (JT) distortions are observed in some perovskite-type $3d$ transition-metal compounds such as KCuF_3 and LaMnO_3 .¹⁻⁴ In the perovskite-type lattice, there are two possible JT distortions depending on the stacking of the elongated octahedra along the c -axis as shown in Fig. 1(a).² In the d -type JT distortion, the elongated axes of the octahedra are parallel along the c -axis. On the other hand, the elongated axes are rotated by 90° along the c -axis in the a -type JT distortion. While LaMnO_3 (d^4), YVO_3 (d^2) and YTiO_3 (d^1) have the d -type JT distortion,^{3,5,6} LaVO_3 (d^2) has the a -type JT distortion.⁷ In KCuF_3 , both the d -type and the a -type JT distortions are observed.² Hartree-Fock calculations which consider the hybridization between the transition-metal $3d$ and oxygen $2p$ orbitals predict that the orbital ordered state compatible with the a -type JT distortion is lower in energy than that with the d -type JT distortion for d^1 and d^2 systems and that the two states are degenerate for d^4 and d^9 systems.⁸ Therefore, one cannot explain why the d -type JT distortion is realized in LaMnO_3 , YVO_3 and YTiO_3 by considering the energy gain due to orbital ordering alone.

Perovskite-type ABO_3 compounds with relatively small A -site ions undergo the GdFeO_3 -type distortion which is caused by tilting of BO_6 octahedra as shown in Fig. 1(b).⁹ While LaMnO_3 , YVO_3 , LaVO_3 and YTiO_3 are accompanied by the GdFeO_3 -type distortion, KCuF_3 has no GdFeO_3 -type distortion. In addition, the magnitude of the GdFeO_3 -type distortion becomes larger in going from LaVO_3 and LaMnO_3 to YVO_3 and YTiO_3 . Here, one can notice that the compounds with the larger GdFeO_3 -type distortion tend to have the d -type JT distortion. It has been pointed out by Goodenough that the covalency between the A -site and oxygen ions (A -O covalency) is important in the GdFeO_3 -type distortion.¹⁰ In this paper, we have studied the relationship between the GdFeO_3 -type and JT distortions considering the A -O covalency and explored the reason why orbital ordering compatible with the d -type JT distortion are favored in

LaMnO_3 , YVO_3 and YTiO_3 in terms of the interaction between the two distortions.

II. METHOD OF CALCULATION

We have employed lattice models for the perovskite-type structure in which the transition-metal $3d$, the oxygen $2p$ and the A -site cation d orbitals are included. The on-site Coulomb interaction between the transition-metal $3d$ orbitals, which is essential to make the system insulating and to cause orbital ordering, are expressed using Kanamori parameters u , u' , j and j' .¹¹ The charge-transfer energy Δ is defined by $\epsilon_d^0 - \epsilon_p + nU$, where ϵ_d^0 and ϵ_p are the energies of the bare transition-metal $3d$ and oxygen $2p$ orbitals and $U (=u-20/9j)$ is the multiplet averaged d - d Coulomb interaction energy. The hybridization between the transition-metal $3d$ and oxygen $2p$ orbitals is expressed by Slater-Koster parameters $(pd\sigma)$ and $(pd\pi)$. The ratio $(pd\sigma)/(pd\pi)$ is fixed at -2.16.¹² Δ , U , and $(pd\sigma)$ can be deduced from cluster-model analysis of photoemission spectra.⁸ Although the error bars of these parameters estimated from photoemission spectra are not so small [$\sim \pm 1$ eV for Δ and U and $\sim \pm 0.2$ eV for $(pd\sigma)$], the conclusions obtained in the present calculations are not changed if the parameters are varied within the error bars.

In the present model, unoccupied d orbitals of the A -site cation such as Y $4d$ and La $5d$ are taken into account. The hybridization term between the oxygen $2p$ orbitals and A -site cation d orbitals is expressed by $(pd\sigma)_A$ and $(pd\pi)_A$. The ratio $(pd\sigma)_A/(pd\pi)_A$ is also fixed at -2.16. The hybridization term between the oxygen $2p$ orbitals is given by $(pp\sigma)$ and $(pp\pi)$ and the ratio $(pp\sigma)/(pp\pi)$ is fixed at -4.¹² It is assumed that the transfer integrals $(pd\sigma)$ and $(pd\sigma)_A$ are proportional to $d^{-3.5}$ and $(pp\sigma)$ is to d^{-2} , where d is the bond length.¹² Without the JT and GdFeO_3 -type distortions, the bond length between two neighboring oxygens and that between the oxygen and the A -site cation are $\sqrt{2}a$, where a is the bond length between the transition-metal ion and the oxygen. $(pp\sigma)$ and $(pd\sigma)_A$ for bond length of $\sqrt{2}a$ are assumed to be

-0.60 and -1.0 eV, respectively.

In the GdFeO₃-type distortion, the four octahedra in the unit cell are rotated by angle of ω around the axes in the (0,1,1) plane in terms of the orthorhombic unit cell. Here, we model the GdFeO₃-type distortion by rotating the octahedra around the (0,1,0)-axis or the b -axis [see Fig. 1(b)]. The subsequent small rotation around the a -axis is required to retain the corner-sharing network of the octahedra. The magnitude of the GdFeO₃-type distortion is expressed by the tilting angle ω around the b -axis. It is important that the A -site ions are shifted approximately along the b -axis to decrease the distance from the A -site ion to the three closest oxygen ions and increase the distance to the three next closest oxygen ions as shown in Fig. 1(b). Here, it is assumed that the shift is along the $(\pm 1/8, 7/8, 0)$ -direction. The magnitude of the shift is proportional to the tilting angle and is assumed to be $\sim 0.05a$, $0.1a$ and $0.15a$ for the tilting angles of 5, 10 and 15°, respectively, which are realistic values for the compounds studied in the present work.^{3,7} As for the Jahn-Teller distortion, it is assumed that the longest bond is by $0.1a$ longer than the shortest bond which is reasonable for LaMnO₃ and is relatively large for LaVO₃ and YTiO₃.^{3,7,6}

III. RESULTS AND DISCUSSION

A. LaMnO₃

In the high-spin d^4 system, in which one of the e_g orbitals is occupied at each site, the A -type antiferromagnetic (AFM) states with $3x^2 - r^2/3y^2 - r^2$ -type orbital ordering with considerable mixture of $3z^2 - r^2$ are predicted to be stable by theoretical calculations^{1,8,13} and are studied by x-ray and neutron diffraction measurements.⁴ Here, the z -direction is along the c -axis. The amount of the $3z^2 - r^2$ component decreases with the JT distortion.⁸ Different ways of stacking the orbitals along the c -axis give two types of orbital ordering: the one compatible with the d -type JT distortion and the other with the a -type JT distortion. These two types of orbital ordering are illustrated in Fig. 2. While, in the orbital ordering of the a -type, the sites 1, 2, 3, and 4 are occupied by $3y^2 - r^2$, $3x^2 - r^2$, $3x^2 - r^2$, and $3y^2 - r^2$ orbitals, the sites 1, 2, 3, and 4 are occupied by $3y^2 - r^2$, $3x^2 - r^2$, $3y^2 - r^2$, and $3x^2 - r^2$ orbitals in the orbital ordering compatible with the d -type JT distortion.

In Fig. 3, the energy difference between the orbital ordered states compatible with the d -type and a -type JT distortions is plotted as a function of the tilting angle of the octahedra, i.e., the magnitude of the GdFeO₃-type distortion. Δ , U , and $(pd\sigma)$ are 4.0, 5.5, and -1.8 eV, respectively, for LaMnO₃.⁸ Without the JT distortion and the shift of the A -site ion, the two states are degenerate within the accuracy of the present calculation (± 1 meV/formula unit cell). This degeneracy is lifted when

the JT distortion is included. With the JT distortion and the shift of the A -site ion, the orbital ordered state with the d -type JT distortion is lower in energy than that with the a -type JT distortion. If we tentatively switch off the shift of the A -site ion and include only the JT distortion, the orbital ordered state with the a -type JT distortion becomes slightly lower than that with the d -type JT distortion as shown in Fig. 3. Therefore, one can conclude that the shift of the A -site ion driven by the GdFeO₃-type distortion is essential to stabilize the orbital ordered state with the d -type Jahn-Teller distortion.¹⁴

The qualitative explanation of this behavior is as follows. In the d -type JT distortion, the four oxygen ions nearest to the A -site ion [shaded in Fig. 1 (a) and (b)] shift approximately in the same direction and, consequently, the system can gain the hybridization energy between the A -site and oxygen ions effectively. On the other hand, in the a -type JT distortion, the two of the four oxygen ions move in the other direction and the energy gain due to the hybridization is small compared to the d -type JT distortion. Another possible picture is that, in the d -type JT distortion, these four oxygen ions can push the A -site ion in the same direction since the JT distortion along the c -axis is in phase. On the other hand, in the case of the a -type JT distortion, the two oxygen ions in the upper plane push the A -site ion in the other direction than the two in the lower plane as shown in Fig. 4. Therefore, the stronger is the GdFeO₃-type distortion, the more does it stabilize the d -type Jahn-Teller distortion and corresponding orbital ordering.

In the charge-ordered state of Pr_{0.5}Ca_{0.5}MnO₃, the Mn³⁺ and Mn⁴⁺ sites are arranged like a checkerboard within the c -plane and the same arrangement is stacked along the c -axis.¹⁵ The Mn³⁺ sites are accompanied by the JT distortion and the elongated axes are parallel along the c -axis just like the d -type JT distortion. Since the A -sites are occupied by Pr and Ca ions in Pr_{0.5}Ca_{0.5}MnO₃, we cannot simply apply the present model calculation to it. However, it is reasonable to speculate that the stacking along the c -axis in Pr_{0.5}Ca_{0.5}MnO₃ is also determined by the interaction between the JT distortion and the shift of the A -site ion in the same way as in LaMnO₃.

B. YVO₃

In the d^2 system, the C -type AFM state in which the sites 1, 2, 3, and 4 are occupied by xy and yz , xy and zx , xy and zx , and xy and yz orbitals and the G -type AFM state in which the sites 1, 2, 3, and 4 are occupied by xy and yz , xy and zx , xy and yz , and xy and zx orbitals are competing. While the C -type AFM state is favored by the orbital ordering which is compatible with the a -type JT distortion, the G -type AFM state is favored by the orbital ordering of the d -type. The relative energy of the G -type AFM state with the d -type

JT distortion to the C -type AFM state with the a -type JT distortion, $E_d - E_a$, is plotted as a function of the tilting angle in Fig. 5. Δ , U , and $(pd\sigma)$ are 6.0, 4.5, and -2.2 eV, respectively, for LaVO_3 and YVO_3 .⁸ Without the GdFeO_3 -type distortion, the C -type AFM state with the a -type JT distortion is lower in energy than the G -type AFM state, indicating that the energy gain due to the orbital ordering is larger in the C -type AFM state than in the G -type AFM state. The energy difference becomes smaller with the tilting or the GdFeO_3 -type distortion. Finally, with the tilting of 15° , the G -type AFM state with the d -type JT distortion becomes lower in energy than the C -type AFM state. The present calculation is in good agreement with the experimental result that the less distorted LaVO_3 is C -type AFM below 140 K⁷ and the more distorted YVO_3 is G -type AFM below 77 K.⁵

This situation is illustrated in Fig. 6. When the GdFeO_3 -type distortion is large, the interaction between the d -type JT distortion and the shift of the A -site ion, namely, the energy gain due to A -O covalency becomes dominant just like in LaMnO_3 and, consequently, the G -type AFM with the d -type JT distortion is favored. On the other hand, when the GdFeO_3 -type distortion is small, the energy gain due to orbital ordering becomes dominant and the a -type JT distortion and the orbital ordering compatible with it are realized. The JT distortion may be suppressed if the system is located near the crossing point where the a -type and d -type JT distortions are almost degenerate. An interesting experimental result related to this point is that YVO_3 becomes C -type AFM between 77 K and 118 K.⁵ The present model calculation suggests that, if the JT distortion is switched off, the C -type AFM state is favored because of the orbital ordering.⁸ Therefore, YVO_3 is expected to be close to the crossing point and become C -type AFM when the d -type JT distortion is suppressed at elevated temperature. In this sense, between 77 K and 118 K, YVO_3 may be an ideal orbitally ordered system without JT distortion.

C. YTiO_3

For the d^1 system, the ferromagnetic (FM) states with orbital ordering are favored in the model HF calculations. There are two possible orbital orderings compatible with the a -type and d -type JT distortions. The model HF calculation without the covalency between the A -site cation and the oxygen ion predicted that the orbital ordering of the a -type is lower in energy. However, the recent neutron diffraction measurement by Akimitsu *et al.* have shown that the orbital ordering compatible with the d -type JT distortion is realized in the FM insulator YTiO_3 .⁶ YTiO_3 has the considerable GdFeO_3 -type distortion and the tilting angle is expected to be larger than 15° . In Fig. 7, the relative energy of the FM and orbital ordered state of the d -type to that of the a -type is plotted as a function of the tilting. Δ , U , and $(pd\sigma)$ are

7.0, 4.0, and -2.2 eV, respectively, for YTiO_3 .⁸ With the tilting of 15° , the orbital ordered state of the d -type is lower in energy, in agreement with the experimental result. In this state, the sites 1, 2, 3, and 4 are occupied by $c_1yz + c_2xy$, $c_1zx + c_2xy$, $c_1yz - c_2xy$, and $c_1zx - c_2xy$ orbitals ($c_1 \sim 0.8$ and $c_2 \sim 0.6$). However, experimentally, less distorted LaTiO_3 has no or very small JT distortion and has a G -type AFM state.¹⁶ The present calculation cannot explain why the G -type AFM state can be stable compared to the FM state in LaTiO_3 .

IV. CONCLUSION

In conclusion, we have studied the relationship between orbital ordering and the JT and GdFeO_3 -type lattice distortions. It has been found that the covalency between the A -site cations and oxygen makes the d -type JT distortion (same orbitals along the c -direction) lower in energy than the a -type JT distortion (alternating orbitals along the c -direction) in the presence of the large GdFeO_3 -type distortion. As a result, the orbital ordered states compatible with the d -type JT distortion are favored in LaMnO_3 , YVO_3 , and YTiO_3 which have the relatively large GdFeO_3 -type distortion. On the other hand, in less distorted LaVO_3 , the orbital ordering compatible with the a -type JT distortion is favored because of the pure superexchange effect.

ACKNOWLEDGMENT

The authors would like to thank useful discussions with K. Tomimoto, J. Akimitsu, Y. Ren and P. M. Woodward. This work was supported by the Netherlands foundation for Fundamental Research of Matter (FOM).

¹ K. I. Kugel and D. I. Khomskii, JETP Lett. **15**, 446 (1972); Usp. Fiz. Nauk. **136**, 621 (1981) [Sov. Phys. Usp. **25**, 231 (1982).]

² A. Okazaki, J. Phys. Soc. Jpn. **61**, 4619 (1969); M. T. Hutchings, Phys. Rev. B **188**, 919 (1969).

³ J. B. Goodenough, Phys. Rev. **150**, 564 (1955); J. B. A. Elemans, B. van Laar, K. R. van der Veen, and B. O. Loopstra, J. Solid State Chem. **3**, 328 (1971).

⁴ J. Rodríguez-Carvajal, M. Hennion, F. Moussa, A. H. Moudden, L. Pinsard, and A. Revcolevschi, Phys. Rev. B **57**, R3189 (1998); Y. Murakami, I. Koyama, M. Tanaka, H. Kawata, J. P. Hill, D. Gibbs, M. Blume, T. Arima, Y. Tokura, K. Hirota, and Y. Endoh, Phys. Rev. Lett. **81**, 582 (1998),

⁵ H. Kawano, H. Yoshizawa, and Y. Ueda, J. Phys. Soc. Jpn. **63**, 2857 (1994).

- ⁶ J. Akimitsu, unpublished.
- ⁷ P. Bordet, C. Chaillout, M. Marezio, Q. Huang, A. Santoro, S-W. Cheong, H. Takagi, C. S. Oglesby, and B. Batlogg, *J. Solid State Chem.* **106**, 253 (1993).
- ⁸ T. Mizokawa and A. Fujimori, *Phys. Rev. B* **51**, 12880 (1995); *Phys. Rev. B* **54**, 5368 (1996).
- ⁹ M. O'Keefe and B. G. Hyde, *Acta Cryst.* **B33**, 3802 (1977); P. M. Woodward, *Acta Cryst.* **B53**, 32 (1997).
- ¹⁰ J. B. Goodenough, *Magnetism and the Chemical Bond*, (New York, 1963); *Prog. Solid State Chem.* **5**, 145.
- ¹¹ J. Kanamori, *Prog. Theor. Phys.* **30**, 275 (1963).
- ¹² W. A. Harrison, *Electronic Structure and the properties of Solids*, (Dover, New York, 1989).
- ¹³ S. Ishihara, J. Inoue, and S. Maekawa, *Phys. Rev. B* **55**, 8280 (1997); L. F. Feiner and A. M. Oleś, unpublished; D. Feinberg *et al.*, *Phys. Rev. B* **57**, R5583 (1998).
- ¹⁴ We have evaluated the Madelung energy of the model perovskite lattices with the JT and GdFeO₃-type distortions and have found that the *a*-type JT distortion is slightly lower in energy than the *d*-type. This is opposite to the effect of the covalency between the *A*-site cations and oxygens.
- ¹⁵ Z. Jirak, S. Krupicka, Z. Simsa, M. Dlouha, and S. Vratilav, *J. Mag. Mag. Mat.* **53**, 153 (1985).
- ¹⁶ J. P. Goral and J. E. Greedan, *J. Mag. Mag. Mat.* **37** 315 (1983).

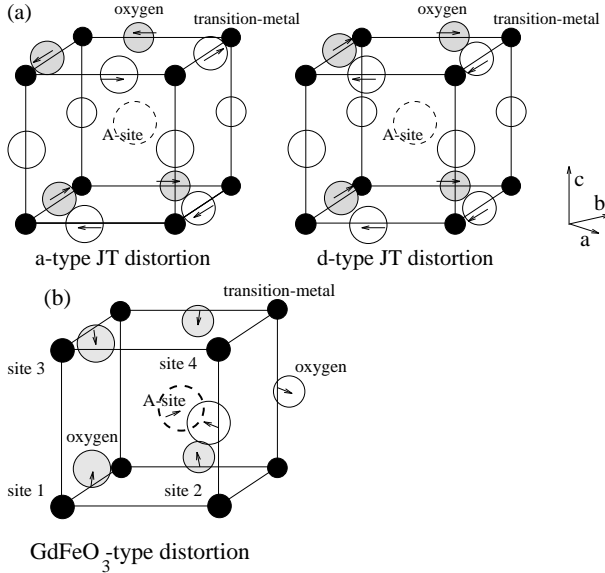


FIG. 1. Schematic drawings for two types of Jahn-Teller distortions (a) and for GdFeO₃-type distortion (b). The arrows indicate shifts of the oxygen and *A*-site ions. In the GdFeO₃-type distortion, the six oxygen ions nearest to the *A*-site ion are shown.

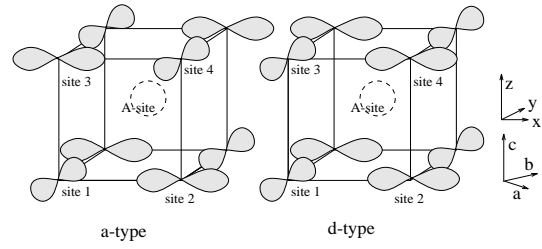


FIG. 2. Two types of orbital ordering for LaMnO₃ compatible with the *a*-type and *d*-type JT distortions.

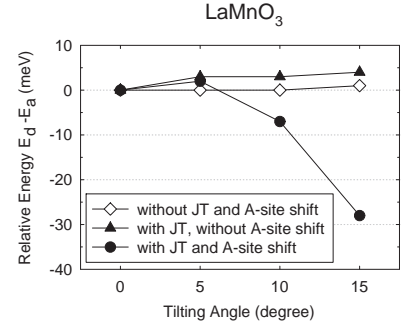


FIG. 3. Energies per formula unit cell of the orbital ordered state compatible with the *d*-type JT distortion relative to that with the *a*-type JT distortion for LaMnO₃ as a function of the tilting angle, i.e., the magnitude of the GdFeO₃-type distortion. closed circles: with the JT distortions and with the shift of the *A*-site cation, open diamonds: without the JT distortions and without the shift of the *A*-site cation, closed triangles: with the JT distortions and without the shift of the *A*-site cation.

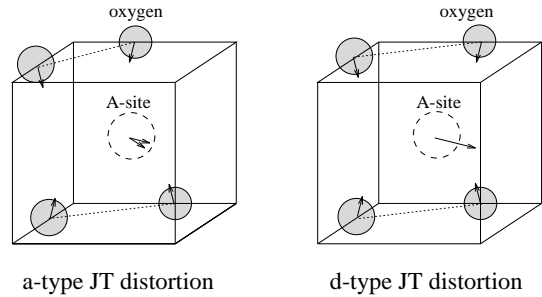


FIG. 4. A rough sketch of the shifts of the oxygen ions and the forces to the *A*-site ion for the *a*-type and *d*-type JT distortions. The oxygen shifts due to GdFeO₃-type distortion are exaggerated. Only the shifts and forces relevant for the present discussion are shown. In the *a*-type JT distortion, the oxygen ions in the upper and lower planes push the *A*-site ion in different directions. In the *d*-type JT distortion, the oxygen ions push the *A*-site ion in the same direction.

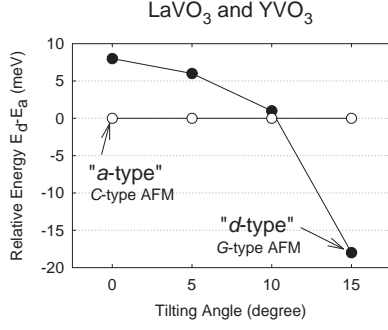


FIG. 5. Energies per formula unit cell of the orbital ordered state compatible with the d -type JT distortion (closed circles) relative to that with the a -type JT distortion (open circles) for YVO₃ and LaVO₃ as a function of the tilting. The shift of the A -site cation is included.

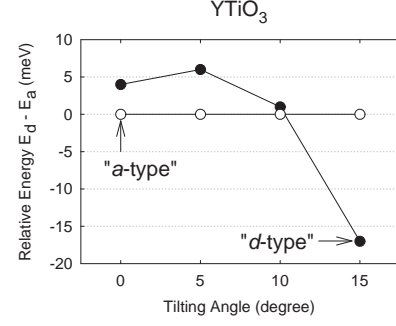


FIG. 7. Energies per formula unit cell of the orbital ordered state compatible with the d -type JT distortion (closed circles) relative to that with the a -type JT distortion (open circles) for YTiO₃ as a function of the tilting. The shift of the A -site cation is included.

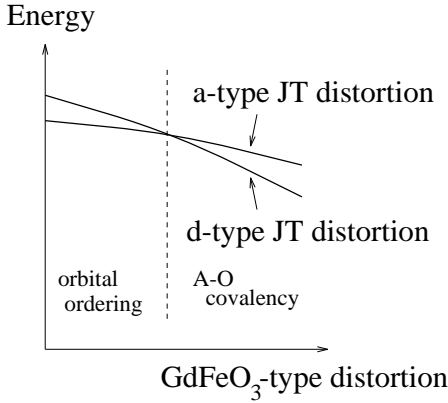


FIG. 6. Energy scheme of the orbital ordered states with the d -type and a -type JT distortions as a function of tilting or the GdFeO₃-type distortion. While, for the small GdFeO₃-type distortion, the energy gain due to the orbital ordering is dominant, the energy gain due to the A -O covalency becomes relevant for the large GdFeO₃-type distortion.